

AD-A061 116

ROME AIR DEVELOPMENT CENTER GRIFFISS AFB N Y
HEAVY ION RADIATION EFFECTS IN VLSI, (U)
MAY 78 J N BRADFORD

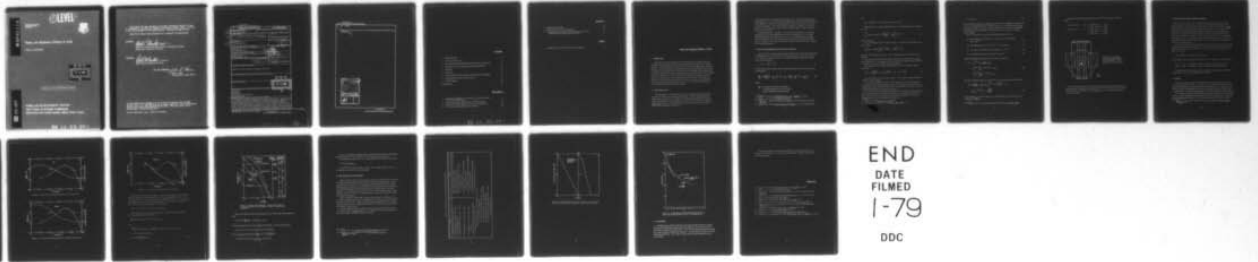
F/G 9/5

UNCLASSIFIED

RADC-TR-78-109

NL

1 of 1
AD
A061 116



END
DATE
FILMED
1-79
DDC

AD A061116

LEVEL III

RADC-TR-78-109
IN HOUSE REPORT
MAY 1978



Heavy Ion Radiation Effects in VLSI

JOHN N. BRADFORD

DDC
RECEIVED
NOV 14 1978
B

FG

Approved for public release; distribution unlimited.

DDC FILE COPY

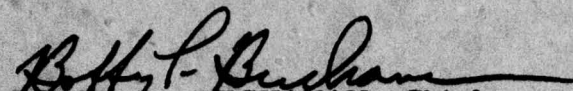
ROME AIR DEVELOPMENT CENTER
AIR FORCE SYSTEMS COMMAND
GRIFFISS AIR FORCE BASE, NEW YORK 13441

78 11 06 004

This report has been reviewed by the RADC Information Office (OI) and is releasable to the National Technical Information Service (NTIS). At NTIS it will be releasable to the general public, including foreign nations.

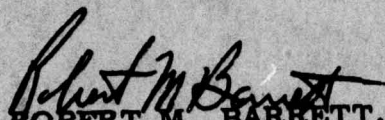
RADC-TR-78-109 has been reviewed and is approved for publication.

APPROVED:



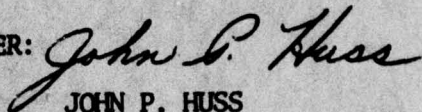
BOBBY L. BUCHANAN, Chief
Radiation Hardened Electronics Technology Branch
Solid State Sciences Division

APPROVED:



ROBERT M. BARRETT, Director
Solid State Sciences Division

FOR THE COMMANDER:



JOHN P. HUSS
Acting Chief, Plans Office

If your address has changed or if you wish to be removed from the RADC mailing list, or if the addressee is no longer employed by your organization, please notify RADC (ESR) Hanscom AFB MA 01731. This will assist us in maintaining a current mailing list.

Do not return this copy. Retain or destroy.

Unclassified

SECURITY CLASSIFICATION OF THIS PAGE (When Data Entered)

REPORT DOCUMENTATION PAGE		READ INSTRUCTIONS BEFORE COMPLETING FORM	
1. REPORT NUMBER 14 RADC-TR-78-199	2. GOVT ACCESSION NO.	3. RECIPIENT'S CATALOG NUMBER	
4. TITLE (and Subtitle) 6 HEAVY ION RADIATION EFFECTS IN VLSI		5. TYPE OF REPORT & PERIOD COVERED In-House	
7. AUTHOR(s) 10 John N. Bradford		8. CONTRACT OR GRANT NUMBER(s) 17 J3	
9. PERFORMING ORGANIZATION NAME AND ADDRESS Deputy for Electronic Technology (RADC/ESR) Hanscom AFB Massachusetts 01731		10. PROGRAM ELEMENT, PROJECT, TASK AREA & WORK UNIT NUMBERS 61102F 23061301	
11. CONTROLLING OFFICE NAME AND ADDRESS Deputy for Electronic Technology (RADC/ESR) Hanscom AFB Massachusetts 01731		12. REPORT DATE 11 May 78	
14. MONITORING AGENCY NAME & ADDRESS (if different from Controlling Office) 12 23p.		13. NUMBER OF PAGES 21	
		15. SECURITY CLASS. (of this report) Unclassified	
15a. DECLASSIFICATION/DOWNGRADING SCHEDULE			
16. DISTRIBUTION STATEMENT (of this Report) Approved for public release; distribution unlimited.			
17. DISTRIBUTION STATEMENT (of the abstract entered in Block 20, if different from Report) DDC			
18. SUPPLEMENTARY NOTES RECEIVED NOV 14 1978 B			
19. KEY WORDS (Continue on reverse side if necessary and identify by block number) Heavy ion Cosmic ray Dosimetry Very large scale integration Microelectronics			
20. ABSTRACT (Continue on reverse side if necessary and identify by block number) Impressive results have been achieved using electron beam, soft x-ray, or synchrotron radiation for lithography and photoresist exposure. Application to microelectronic circuitry paved the way for Very Large Scale Integration (VLSI) in which device sizes of micron and submicron dimension are forecast. This small size presents new problems for radiation effects test and assessment. One example is the interaction of heavy ions (namely, cosmic rays) with a VLSI size device and the associated nonequilibrium dosimetry involved. This report treats the case of VLSI exposure in satellite environment. The numbers			

DD FORM 1 JAN 73 1473

EDITION OF 1 NOV 65 IS OBSOLETE

Unclassified

SECURITY CLASSIFICATION OF THIS PAGE (When Data Entered)

309 050

next page
LW

Unclassified

SECURITY CLASSIFICATION OF THIS PAGE(When Data Entered)

20. (Cont)

suggest that very small size is not a desirable feature for devices in that environment.

ACCESSION for	
NTIS	White Section <input checked="" type="checkbox"/>
DDC	Buff Section <input type="checkbox"/>
UNANNOUNCED	<input type="checkbox"/>
NOTIFICATION	
BY	
DISTRIBUTION/AVAILABILITY CODES	
Dist. AVAIL. and/or SPECIAL	
A	

Unclassified

SECURITY CLASSIFICATION OF THIS PAGE(When Data Entered)

Contents

1. INTRODUCTION	5
2. DEVICE SIZES IN VLSI	5
3. SIZE AND DOSE DISTRIBUTIONS NEAR HEAVY ION TRACKS	6
4. STATISTICS OF THE ENERGY DEPOSITION PROCESS	10
5. SOURCES	10
6. EFFECTS	11
7. INTERACTION CROSS SECTION AND ENERGY DEPOSITION	12
8. SIMULATION OF HEAVY ION EFFECTS	16
9. CONCLUSIONS	19
REFERENCES	20

Illustrations

1. Radial Dose Distribution Around Heavy Ion Track Normal to Plane of an MOS Device	9
2. LET and Free Space Spectrum For Fe ⁵⁶ Cosmic Rays	13
3. LET and Free Space Spectrum For Carbon Cosmic Rays	13
4. LET and Free Space Spectrum For Protons	14

Illustrations

5. Integral LET Spectrum	15
6. Differential Free Space LET Spectra	18
7. Comparison of Radial Distributions For Heavy Ions, SEM Electron Beams, Theory, and Experiment	19

Tables

1. Comparison for Various Parameters of Simulation	17
----------------------------------------------------	----

Heavy Ion Radiation Effects in VLSI

1. INTRODUCTION

Nonuniform distribution effects show up dramatically in dosimetry when the dimensions of the region of interest are approximate to the ranges of the electrons involved. Recent development of interface dose enhancement phenomena attests to that fact. In the continuing size reduction associated with microelectronic circuitry a dimension is being approached in which uniform dose testing will be inappropriate to specify response on hardness. The electrons generated by heavy ion (for example, cosmic ray) traversal are a case in point. The ion-electron collisions generate a flux with $\sim 1/E^2$ spectrum and maximum energy of about 10 keV. The range in silicon of a 10 keV electron is 1.4 microns. Thus, when microelectronic devices reach this size, local dose anomalies can occur. Very Large Scale Integration (VLSI) crosses the threshold into this domain.

2. DEVICE SIZES IN VLSI

LSI technology has increased the density of circuit elements to about 70,000 per chip with a device size of about 1-mil square. Present masking techniques (optical) lead to edge acuities of 2500 Å. This means that the intradevice dimensions are greater than a few microns ($25 \mu = 1 \text{ mil}$). As a result, the energy deposition profile normal to an energetic heavy ion track occupies an area small in

(Received for publication 18 May 1978)

comparison with device element cross sectional areas. Hence, a single ion track cannot influence a device of LSI dimensions except in the most contrived and extreme circumstances.¹ This is due to the fact that the energy loss mode of a heavy ion is electron collisions. That collision process produces a spectrum of electrons which has a few members of energy > 10 keV and the range of a 10 keV electron in silicon is 1.4 microns.²

In consequence of the foregoing, a dramatic effect of single heavy ion energy deposition will not become apparent until device sizes approach 1 or 2 microns. This situation will occur with the advent of VLSI. The projections are for edge acuties of 50 Å that could lead to element sizes of several hundred Å and devices about 1 μ on edge.³ The transition is made possible by use of soft x-ray or electron beam masking techniques.

3. SIZE AND DOSE DISTRIBUTIONS NEAR HEAVY ION TRACKS

When a fast heavy ion penetrates condensed matter some of the orbital electrons are stripped from the ion and a beam of such ions then has a mean ionic charge, $z \leq Z$; z has been measured widely as a function of energy and velocity of the ion and is given by Barkas⁴

$$z = Z(1 - e^{-125 \beta Z^{-2/3}}) \quad (1)$$

The ion loses energy through electron collisions and generates an electron flux at a rate given by

$$\frac{dn}{d\omega} = \frac{2\pi N z^2 e^4}{mv^2} \cdot \frac{1}{\omega^2} \left[1 - \beta^2 \omega/\omega_m + \frac{\pi \beta z}{137} \left(\frac{\omega}{\omega_m}\right)^{1/2} \left(1 - \frac{\omega}{\omega_m}\right) \right] \quad (2)$$

where

$$\frac{dn}{d\omega} = \text{the number of electrons of energy } \omega, \\ \omega + d\omega \text{ generated per cm of ion track in} \\ \text{matter containing } N \text{ electrons/cm}^3.$$

1. Binder, D. et al (1975) IEEE Trans. Nuc. Sci. NS-22(No. 7):2675.
2. Ashley, J. C. et al (1966) RADC-TR-76-125.
3. Holton, W. C. (1977) The large scale integration of microelectronic circuits, Sci. Am.
4. Barkas, W. H. (1963) Nuclear Research Emulsions, Vol. I Academic Press.

and

$$\omega_m = 2 m c^2 \beta^2 \gamma^2 e, m \text{ are electron charge, mass.}$$

Integration of this equation yields the number of electrons between two energies W_1, W_2 ,

$$\int_{W_1}^{W_2} dn/d\omega = 2\pi N (e^2/mc^2)^2 \left[\frac{mc^2}{W_1} - \frac{mc^2}{W_2} \right] z^2/\beta^2 \quad (3)$$

(see Reference 5).

Thus, the integral spectrum falls off like $\frac{1}{W}$. Evaluation of the integral above 5 keV yields

$$\int_5^{\infty} dn/d\omega = 2\pi N \left(\frac{e^2}{mc^2} \right)^2 \left[\frac{mc^2}{5} - \frac{mc^2}{\infty} \right] z^2/\beta^2$$

which for Fe^{56} cosmic rays with $\beta = 0.5$ in silicon gives 4.3×10^5 electrons/centimeter.

Thus in a slab of Si 1500 Å thick only 6 electrons are liberated with energies greater than 5 keV. The range of a 5 keV electron in Si is 4400 Å so the electrons are confined to a radius < 4400 Å (ignoring diffusion).

The energy loss rate in the target is obtained from the Livingston-Bethe formalism

$$dE/dx = \frac{4\pi e^4 Z^2}{m v^2} N Z_m \left[\ln \frac{2m v^2}{I} - \ln(1 - \beta^2) - \beta^2 \right]. \quad (4)$$

For Fe^{56} cosmic rays this can be ~30 Ge V/cm so that in a slab 1500 Å thick ~450 keV could be dumped.

A much less probable but more dramatic energy loss occurs in the nuclear reactions that can result (p, n; p, 2n; p, α , etc.). When protons or α particles are the projectile, these reactions lead to "star" reactions that can deposit much more ionizing energy locally than the primary proton.

The above electron generation mechanisms can be coupled with electron transport models to produce a relatively detailed picture of the dose and electron flux near a heavy ion track. Katz⁶ has made extensive calculations of the energy deposited near an ion track with the following result:

5. Mott, N. (1929) Proc. Roy. Soc. 124-425.

6. Kobetich, E., and Katz, R. (1968) Phys. Rev. 170, No. 2.

$$D = kz^2/r^2, \quad (5)$$

that is the energy deposition in ergs/g at radius r from a cylindrical track falls off as $1/r^2$ and is proportional to z^2 , where from above, z is the mean ionic charge of the ion or cosmic ray. Both z and k are functions of β . Recent measurements at Brookhaven⁷ have verified the $1/r^2$ dependence over a range of 1 to 300 nm (10 Å to 3000 Å).

The $1/r^2$ character can be developed approximately as follows:

$$(1) \text{ The initial electron spectrum is created with } 1/E^2 \text{ probability} \\ \phi(E) = \phi_0/E^2, \quad (6)$$

$$(2) \text{ The stopping power } dE/dx = k/E^{0.7} \text{ at low energies,} \quad (7)$$

$$(3) \text{ The range of an electron at low energies, } R = KE^{1.7}, \quad (8)$$

$$(4) \text{ The electron attenuation rate is } \phi(r) = \phi_0 e^{-r/R}, \quad (9)$$

Therefore the total energy loss rate at a radius r is given by

$$\begin{aligned} dE &= - \int_0^{E_{\max}} \phi(r, E) \frac{dE}{dx} dE dr, \\ &= - \int_0^{E_{\max}} \frac{\phi_0}{E^2} e^{-r/R} k/E^{0.7} dE dr, \\ &= - \int_0^{E_{\max}} \frac{k\phi_0}{E^{2.7}} e^{-r/KE^{1.7}} dE dr. \end{aligned} \quad (10)$$

The dose (energy deposited in a shell dr thick divided by the mass of the shell)

$$\begin{aligned} D(r) &= \frac{dE}{2\pi r \rho dr} = \frac{1}{2\pi r \rho} k\phi_0 \int_0^{E_{\max}} (-) \frac{e^{-r/KE^{1.7}}}{E^{2.7}} dE, \\ &= \frac{L}{r^2} e^{-r/R_{\max}} \quad L = \frac{+kK\phi_0}{2\pi\rho}. \end{aligned} \quad (11)$$

hence since R_{\max} is of the order of 1 μ , $D(r)$ will follow as $1/r^2$ for the first fraction of a micron.

7. Varma, M. N. et al (1977) Radial dose for O^{16} in N_2 . Rad. Res. 70:511.

In particular the dose profile in quartz for Fe^{56} cosmic rays (see Figure 1) shows

- | | |
|-----------------------|-----------------------------------------------------|
| (a) at $\beta = 0.02$ | $D = 1.4 \times 10^{10}$ rad at $r = 4 \text{ \AA}$ |
| | 7×10^7 rad at $r = 160 \text{ \AA}$ |
| (b) at $\beta = 0.1$ | $D = 7 \times 10^8$ rad at $r = 4 \text{ \AA}$ |
| | 7×10^4 rad at $r = 1400 \text{ \AA}$ |
| | 7×10^2 rad at $r = 1.4 \mu$ |

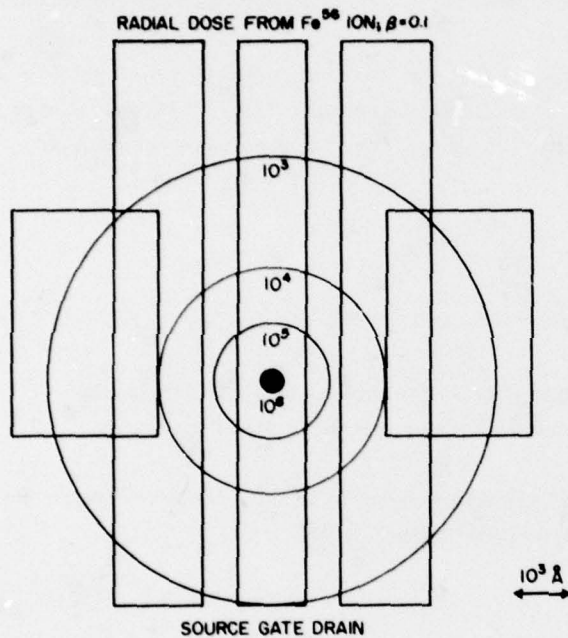


Figure 1. Radial Dose Distribution Around Heavy Ion Track Normal to Plane of an MOS Device. VLSI dimensions are approximate

Thus, the picture that describes the generated electron energy deposition is an intense central core $\sim 20 \text{ \AA}$ in radius with doses $\sim 10^{7-10}$ rad for heavy ions and 10^6 rad for protons and mesons, that dose falling off as r^{-2} with a 100 rad radius of about 1μ in silicon.

4. STATISTICS OF THE ENERGY DEPOSITION PROCESS

When a heavy ion traverses a target the total energy loss is the sum of the individual electron collision losses. If the number of collisions is large and the total energy loss is large compared to the maximum loss to an electron in a single encounter, then the energy loss distribution is a gaussian. If not, if the total collision loss is comparable to the maximum single loss, then the distribution is skewed by the weight of improbable but large energy loss single collisions and a distribution described by Landau, Vavilov or Symon results. Thus, in computing the energy loss of a heavy energetic ion traversing a thin target, one must take care to include the production of energetic delta rays and not simply use the continuous slowing down approximation.

Since it is the high energy electrons that are rarely produced, one must use the appropriate statistics to describe them. The generation rate of electrons of energy greater than some E_0 is given by Eq. (3). If one takes this as the average rate (delta rays/cm) is

$$P(n) = \frac{e^{-M}}{n!} M^n \text{ where } M \text{ is the Mott}^5 \text{ result.}$$

For example, in the case described in Section 2, $M = 6$ electrons (> 5 keV/1500 Å)

$$\begin{aligned} P(6) &= 0.13 \quad \text{for example, one gets 6 electrons only 13\% of the cases,} \\ P(10) &= 0.05 \quad \text{for example, one gets 10 electrons in 5\% of the cases.} \end{aligned}$$

The point here is that the actual yield is subject to considerable variation and using only the mean value misrepresents the situation.

5. SOURCES

Sources of fast heavy ions are the naturally occurring fluxes in space and the man-made accelerated variety. The cosmic, solar, and trapped earth protons and ions have been studied and measured but not in elaborate detail. The proton component varies due to magnetospheric and solar activity and is hard to describe with a single profile. The heavier components are reasonably stable and quite energetic.⁸

For radiation effects purposes the fluxes and energy profiles seem well enough known to make calculations on the number of events to be expected in a satellite due to natural background of cosmic rays. At least one attempt is in the IEEE literature.¹

8. Apparao, M. M. V. (1975) Components of cosmic radiation, Topics in Astro Physics, Vol. 11.

The fluxes of particles can be made into 5 groups: protons; α particles (He); C, O, N; Mg, Si; Fe, Ni, Co. Protons constitute ~90% of the total flux; He about 9%. The LET rates range up to 30 GeV cm²/g. The energies of the most energetic 10% are greater than 1 GeV/nucleon, sufficient to penetrate one to several inches of aluminum.

Manmade fluxes can be generated by a variety of accelerators. Proton linacs capable of intense beams of 1 GeV are in operation and the Berkeley Bevalac has recently achieved 1 GeV/nucleon Fe⁵⁶ beams.

The cosmic fluxes can be evaluated by their kerma as follows:

$$\text{Dose} = k \int \frac{dN}{dE} \frac{dE}{dx} \cdot dE,$$

$$\frac{dN}{dE} \text{ in particles/cm}^2 \text{ MeV}, \quad \frac{dE}{dx} \text{ in MeV cm}^2/\text{gm},$$

$$K = 1.6 \times 10^8 \text{ rad/g/MeV}.$$

This has been done for tissue with the following results:⁹

		<u>Dose rate rad/year</u>
Proton	Z = 1	4.6
He ion	Z = 2	3.5
M ion	6 ≤ Z ≤ 9	1.9
LH ion	10 ≤ Z ≤ 14	1.3
VH ion	26 ≤ Z ≤ 28	1.3

6. EFFECTS

The effects of fast heavy ion energy loss are the same as routinely encountered in radiation hardening; pseudo permanent damage (for example, displacement, oxide, and insulator charge up) and transient (induced conductivity, electron-hole pair creation, diffusion, and collection). In that sense the description is unchanged. What is different has already been alluded to in the determination of the sizes of the affected areas. The following differences occur:

- (a) Higher doses than any proposed for hardness are achieved in the central core of an ion track. Higher by three orders of magnitude for heavy ions (Fe).
- (b) In the natural background case, the doses are delivered randomly in time and location in the satellite,

9. Curtis, S. B. (1976) IEEE Trans. Nuc. Sci. NS-23-1355-1360.

- (c) Average doses due to cosmic background are trivially small yet each individual event which would cause no effect in SSI, May trigger LSI circuit response (see Binder *iff*) or potential annihilation of a circuit element in VLSI.
- (d) The decrease in size of a circuit element leads to smaller probability of heavy ion hit, but the purpose of VLSI is to increase the total number of circuits in the same proportion, hence the "target" area remains fixed.
- (e) Threshold effects (charge required to flip-flop, death of biological cell, charge release needed for dielectric breakdown) can appear which would never be seen in total dose scenario. As an example, if a local energy dump ΔE is required for threshold event then $\Delta E/\Delta m$ is local dose required. If that dose were say 10^8 rad, one could irradiate with low energy electrons or photons right up to 10^8 rad and see no events. However, every heavy ion which passes through Δm (for small Δm) can create events even though average total dose is near zero. In this way total dose hardening concepts fail and must be replaced with a microdose distribution concept.
- (f) These effects occur without a nuclear warfare scenario.
- (g) These effects could become dominant in a star wars scenario (ion beam weapons, satellite-satellite encounters, flooded phase space injection with fast heavy ions).

7. INTERACTION CROSS-SECTION AND ENERGY DEPOSITION

Without performing detailed calculations one can still scope the cosmic ion interaction problem from the available literature. Figures 2 to 4 show composites of the particle spectra for protons, carbon, and iron and their respective LET's as a function of energy/nucleon. These results are taken from References 9 and 10.

Figure 5 shows the integral over all cosmic species for LET > LET vs LET. For instance, there are 250,000 particles/cm²·year with LET > 100 MeV cm²/g. The effect of 20 g/cm² of shielding (3.4-in. Al) is also shown.

10. Heinrich, W. (1977) Rad. Effects 34:143-148.

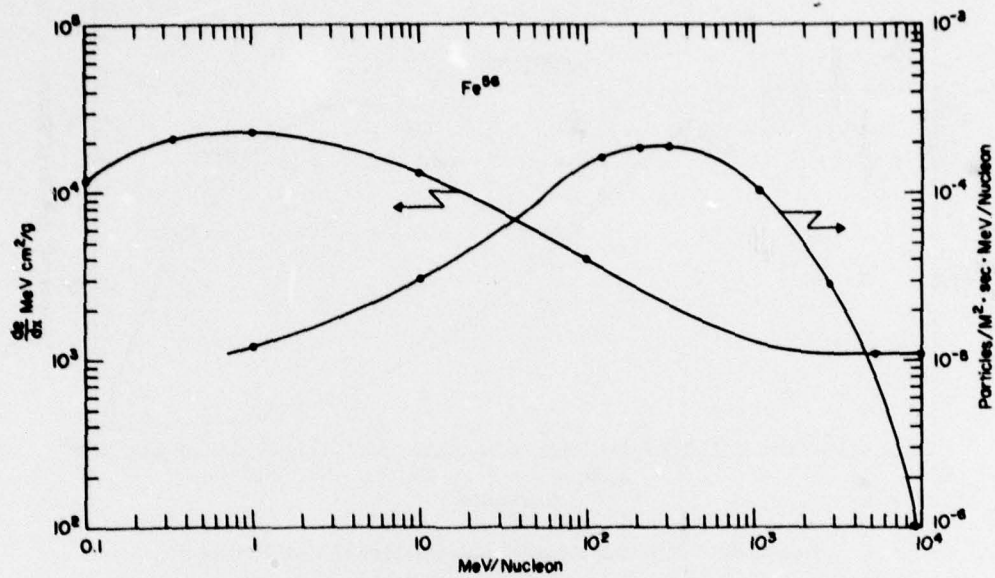


Figure 2. LET and Free Space Spectrum For Fe⁵⁶ Cosmic Rays

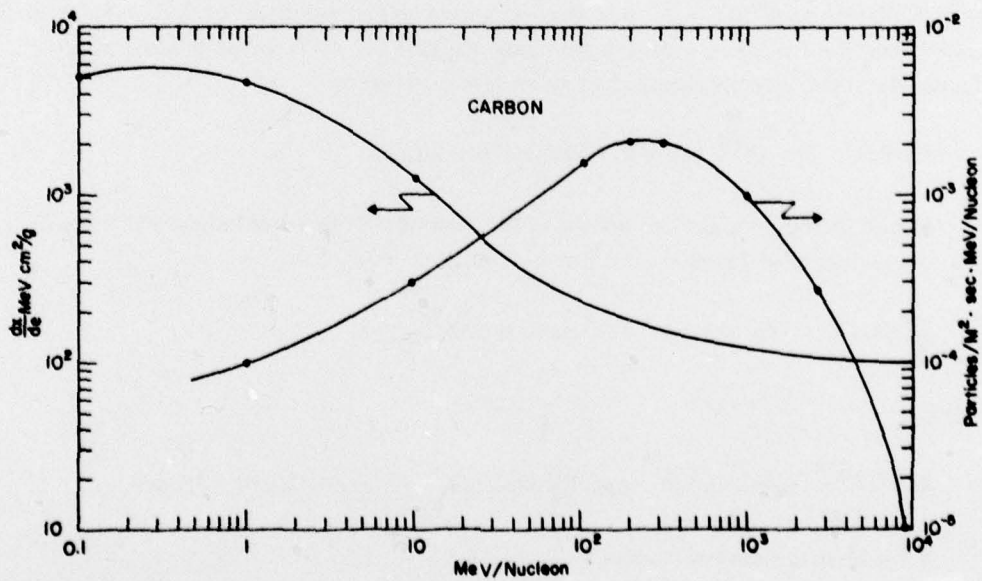


Figure 3. LET and Free Space Spectrum For Carbon Cosmic Rays

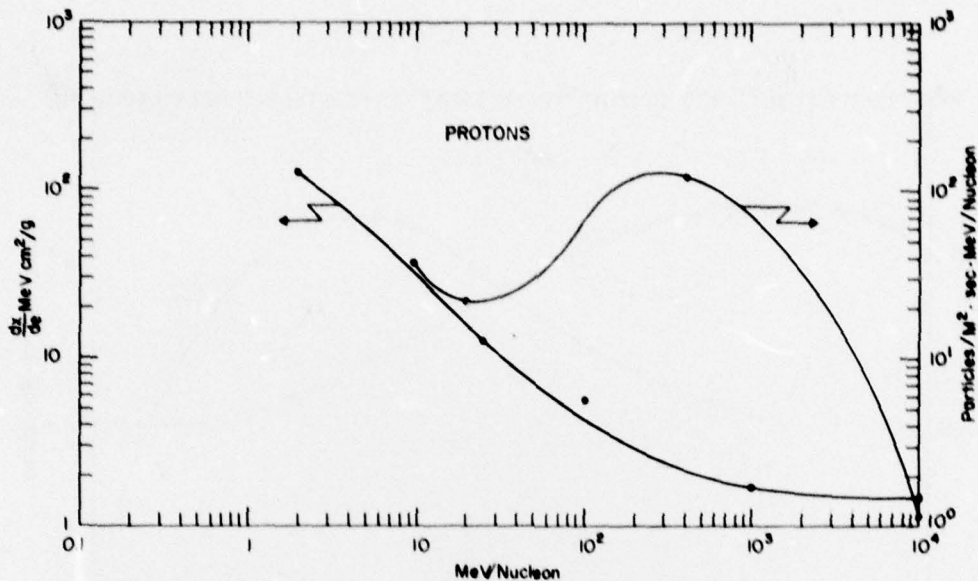


Figure 4. LET and Free Space Spectrum For Protons

In the first vertical column of Figure 5 is the number of hits on assumed VLSI sensitive volumes in a typical chip, 0.2 cm on edge containing 10^6 devices. The area/chip is $4 \times 10^6 \mu^2$ ($4 \mu^2$ per device) with a depletion depth of 2μ . The average chord length for a convex device (the gate region) $1 \times 2 \times 0.2 \mu$ is 0.3 microns. Thus, the mean energy deposition by an ion is given by

$$\text{LET} \times 0.3 \times 10^{-4} \text{ cm} \times 2.33 \text{ g/cm}^3 \text{ for silicon.}$$

These energy dumps are shown in the second and third columns of Figure 5. The computation proceeded as follows:

$$\frac{dE}{dx} \text{ MeV cm}^2/\text{g} \times \text{g/cm}^3 \times \bar{s} \text{ cm} = E \text{ MeV.}$$

Also,

$$\frac{1.6 \times 10^{-8}}{V} \text{ ergs/100 g} \cdot \text{MeV} \frac{dE}{dx} \text{ MeV cm}^2/\text{g} \times \text{g/cm}^3 \times \bar{s} \text{ cm} = D \text{ rad.}$$

$$\bar{s} = 4 V/A \text{ for convex bodies.}$$

$$1.6 \times 10^{-8} \frac{dE}{dx} \frac{\rho \cdot 4 \cdot V}{\rho \cdot V \cdot A} = D. \quad (14)$$

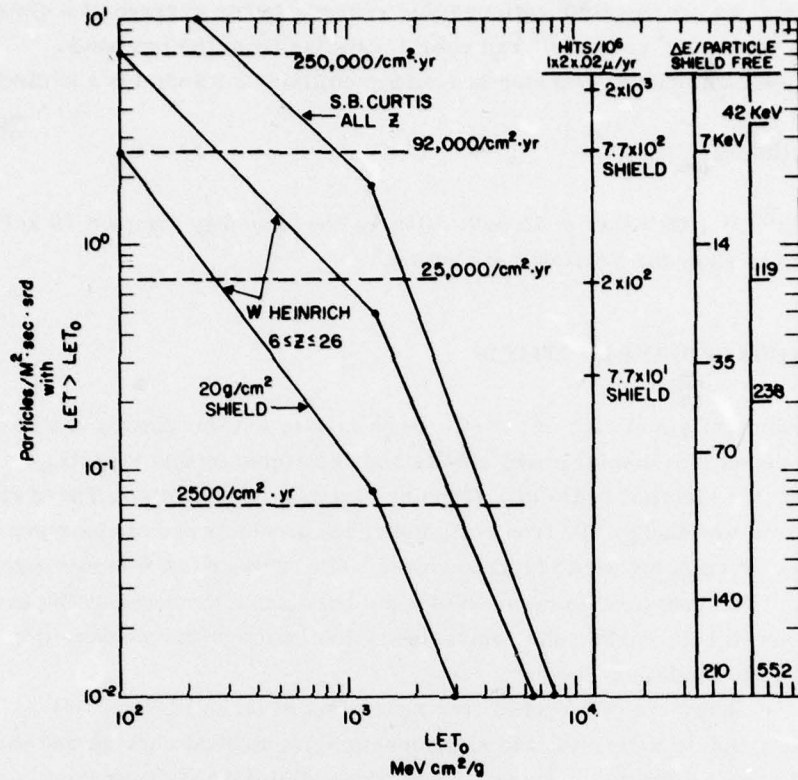


Figure 5. Integral LET Spectrum. Columns show hits and energy deposition in VLSI sensitive volumes of assumed size (see text)

Thus, the average dose from each particle to any convex object can be obtained from:

$$1.6 \times 10^{-8} \cdot \frac{dE}{dx} (\text{MeV cm}^2/\text{g}) \cdot \frac{4}{A} = D \text{ rad.}$$

A is the total surface area, not projected cross section. For the example above

$$A = 2(2 \times 1 + 1 \times 0.2 + 2 \times 0.2) \mu^2 = 5.2 \times 10^{-8} \text{ cm}^2,$$

and for a maximum LET particle $\frac{dE}{dx} = 6.5 \times 10^3 \frac{\text{MeV cm}^2}{\text{g}}$

$$1.6 \times 10^{-8} \times 6.5 \times 10^3 \times \frac{4}{5.2 \times 10^{-8}} = 8 \times 10^3 \text{ rad.}$$

However, as previously mentioned this represents the average of a distribution that varies from $\sim 10^9$ rad to 10^2 rad over 1 μ radius from the ion track.

The maximum energy transfer in a single collision between ion and electron is

$$E = 4 (me/M_{ion}) E_{ion}.$$

For Fe^{56} at 1 GeV this is 35 keV. Hence, those energy dumps ≤ 70 keV can be expected to show the Vavilov distribution.

8. SIMULATION OF HEAVY ION EFFECTS

Experimental simulation of the effects of cosmic ion irradiation can be achieved to a large extent (not displacement effects and restricted to thin targets, $t < \text{few microns}$) by the electron beam in a scanning electron microscope. Those effects deriving from low energy electron collisions such as electron-hole pair production and subsequent trapping would be reproduced well. Others, some more lethal, would not. (For instance the creation of a pin hole punch through leading to a gate-substrate short.) In Table 1 the comparisons are indicated for various important parameters of simulation.

Figure 6 shows the differential free space flux of large LET particles. One can use the graph to determine the relationship between SEM current and the cosmic ray flux at each LET rate. Figure 7 shows the radial dose profiles from a SEM operated at 10 and 20 keV as computed by Chadsey¹¹ and the previously mentioned work of Katz⁶ and of Varma.⁷

Galloway and Poitman¹² have indicated the pertinent parameters for an SEM as a device to deliver uniform exposure to LSI/MOS devices, but nonuniformity is the characteristic of radiation effects in the small.

11. Chadsey, W. L. (1973) NAD Crane Technical Report 7024-C74-69.

12. Galloway, K., and Poitman, P. (1977) IEEE Trans. Nuc. Sci.
NS-24(No. 6):2066.

Table 1. Comparisons for Various Parameters of Simulation

IONS	SEM
<ol style="list-style-type: none"> 1. Radial Dose from Track $D = k z^2 / r^2$ 2. Central highly ionized core 20 Å radius 3. Dose proportional to z^2 4. dE/dx for ion from 10^4 to 1 MeV cm^2/g 5. dE/dx constant over interaction range 6. Ion impacts to occur randomly in space and time 7. Highest energy secondary expected ~40 keV, secondaries distributed like $1/E^2$ 	<ol style="list-style-type: none"> Radial Dose from Beam Center $D = k/r^2$ (See Figure 7) Beam spot diameter 50 to 100 Å Beam current adjustable for any z dE/dx for 60 keV electron 4 MeV cm^2/g Use intensity to scale dE/dx slowly varying over interaction range Limit thickness of target Normal raster can be programmed using triggered on pulses to blanking coil High energy secondary = 1/2 primary energy, secondaries distributed like $1/E^2$
<p>Probable modifications on an existing SEM would be:</p> <ol style="list-style-type: none"> (1) Fast pulses to blanking coil, (2) Primary energy in the 30 to 60 keV range, (3) Ability to measure very small beam currents, (4) Focussing to 50 Å - 100 Å diameter, (5) Test gear and chamber modification to permit device response readout. 	

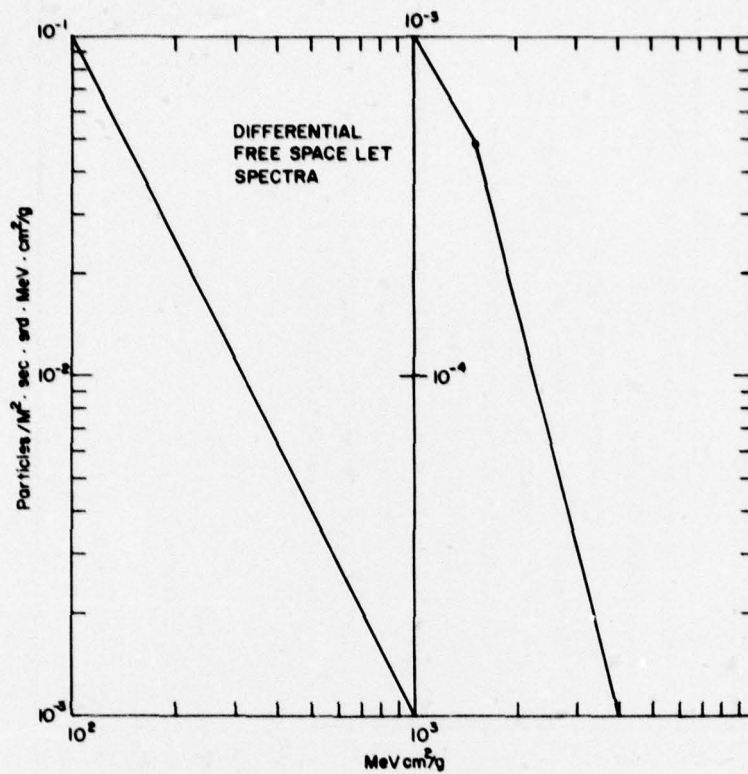


Figure 6. Differential Free Space LET Spectra. Ordinate gives total number of particles (all groups) with common LET value

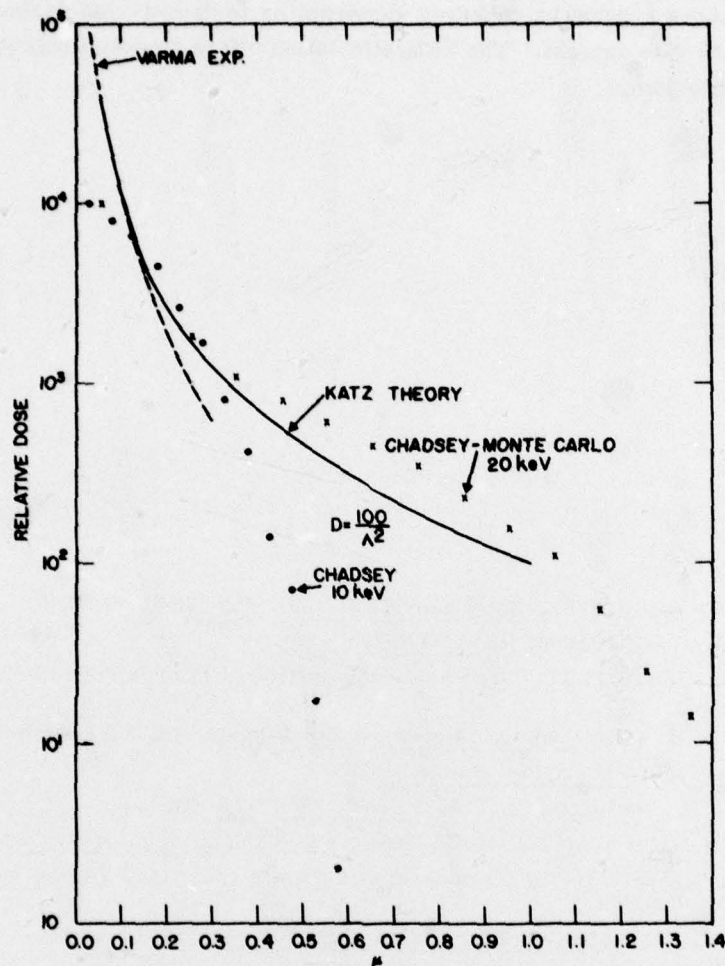


Figure 7. Comparison of Radial Distributions For Heavy Ions, SEM Electron Beams, Theory, and Experiment

9. CONCLUSIONS

Nonequilibrium dosimetry effects become apparent when regions of interest (devices) have dimensions approximate to the ranges of the electrons involved. Total dose concepts fail in that domain. VLSI radiation effects testing and analysis will require elevated sensitivities amongst the radiation effects community to cope with these phenomena. The cosmic ray interactions in space applications are a case in point.

The numbers suggest an enhanced vulnerability to damage and device mode change in VLSI size devices. The SEM simulation offers a partial solution to the assessment problem.

References

1. Binder, D. et al (1975) IEEE Trans. Nuc. Sci. NS-22(No. 7):2675.
2. Ashley, J. C. et al (1966) RADC-TR-76-125.
3. Holton, W. C. (1977) The large scale integration of microelectronic circuits, Sci. Am.
4. Barkas, W. H. (1963) Nuclear Research Emulsions, Vol. I Academic Press.
5. Mott, N. (1929) Proc. Roy. Soc. 124:425.
6. Kobetich, E., and Katz, R. (1968) Phys. Rev. 170, No. 2.
7. Varma, M. N. et al (1977) Radial dose for O^{16} in N_2 , Rad. Res. 70:511.
8. Apparao, M. M. V. (1975) Components of cosmic radiation, Topics in Astro Physics, Vol. 11.
9. Curtis, S. B. (1976) IEEE Trans. Nuc. Sci. NS-23:1355-1360.
10. Heinrich, W. (1977) Rad. Effects 34:143-148.
11. Chadsey, W. L. (1973) NAD Crane Technical Report 7024-C74-69.
12. Galloway, K., and Poitman, P. (1977) IEEE Trans. Nuc. Sci. NS-24(No. 6):2066.